

Synthesis, Electrochemical and Optical Properties of Ru^{II}-Diphenylphenanthroline–Ethylnylpyrenephenanthroline Systems

Christine Goze,^[a] Cristiana Sabatini,^[b] Andrea Barbieri,^[b] Francesco Barigelletti,^{*[b]} and Raymond Ziessel^{*[a]}

Keywords: Ruthenium / Pyrenes / Energy conversion / Electrochemistry / Photophysics

The synthesis, electrochemical and optical spectroscopic properties of a Ru^{II}-diphenylphenanthroline complex decorated with ethynylpyrene (EP) appendages, **1**, and those of its parent bromo-substituted complex, **2**, are reported; complex **1** is [Ru(dpp)₂(phen-EP₂)](PF₆)₂ and **2** is [Ru(dpp)₂(phen-Br₂)](PF₆)₂, where dpp is 4,7-diphenyl-1,10-phenanthroline, phen-EP is 5,6-(1-ethynylpyrene)-1,10-phenanthroline and phen-Br₂ is 5,6-dibromo-1,10-phenanthroline. In CH₃CN solvent, both bromo- and EP-substituted complexes are redox active and metal-centred and ligand-centred processes are assigned with reference to the analogous steps for [Ru(phen)₃]²⁺ and to steps for the EP appendages. The complexes exhibit strong absorption bands in the near-UV and visible regions due to ligand-centred (LC) and metal-to-ligand charge-transfer (MLCT) transition, respectively. For **1**, the lowest-lying absorption band is slightly redshifted due to better delocalisation at the phen-EP ligand. At room tem-

perature and in O₂-free solvent, complex **1** appeared to be practically nonluminescent, whereas **2** exhibited intense ³MLCT emission; quantum yields of $f_{em} = 9 \times 10^{-4}$ and 6.1×10^{-2} were found for **1** and **2**, respectively and $\lambda_{exc} = 462$ nm in both cases. The lowest-lying excited states of **1** were assigned as ³LC states, which were localised on the EP moiety. These states are nonluminescent, which thus explains the weak room-temperature luminescence for this complex. At 77 K, **2** is emissive, as expected for ³MLCT levels; however, a moderately intense ³MLCT emission was also observed for **1** at this temperature. For the latter case, this outcome is tentatively explained in terms of local trapping of ³MLCT states at the 4,7-diphenylphenanthroline ligands free of EP appendages.

(© Wiley-VCH Verlag GmbH & Co. KGaA, 69451 Weinheim, Germany, 2008)

Introduction

Within light energy conversion schemes, Ru^{II}-polypyridine units are useful components of assemblies designed for the photogeneration of energy and electron-transfer processes.^[1] A number of model molecular wires, dyads, triads and dendritic multicomponent systems incorporate such units, and their optical absorption and emission properties have been extensively investigated.^[2,3] Remarkably, the luminescence lifetime of some Ru^{II}-polypyridine emitters can be conveniently tuned as a consequence of excited state equilibration processes, wherein organic counterparts are involved.^[4] Out of the various organic units employed, which are appended to the ligands of the first coordination sphere, pyrene has proved to be quite effective in the tuning process of Ru^{II}-tris(bichelating) emitters, namely [Ru(bpy)₃]²⁺, where bpy is 2,2'-bipyridine.^[5] Reasons are

that upon light absorption (either by the transition-metal chromophore or by the pyrene unit), the final population of interacting metal-to-ligand charge-transfer and ligand-centred triplets, ³MLCT and ³LC, respectively, takes place.^[6] In most cases, these are localised at the transition metal and at the pyrene components, respectively, with the ³LC (pyrene) level lying only a few hundreds of wavenumbers below the ³MLCT level.

Along these lines of investigation, we prepared the new phen-EP₂ ligand and two complexes: a bichromophore, [Ru(dpp)₂(phen-EP₂)]²⁺ (**1**) and its parent disubstituted dibromophenanthroline species (**2**), where dpp is 4,7-diphenyl-1,10-phenanthroline and EP is ethynylpyrene (Schemes 1 and 2). In **1**, the Ru-based component is a heteroleptic system containing dpp and 1,10-phenanthroline ligands (phen), and the latter contains two EP appendages. These are designed to influence the photophysics of the Ru-dpp core; for the reference complex [Ru(dpp)₃]²⁺, the room-temperature luminescence quantum yield, f_{em} , ≈ 0.4 ,^[7-9] is six times higher than that of [Ru(bpy)₃]²⁺, f_{em} , ≈ 0.06 .^[10] We examined the excited-state dynamics of this complex and found that the lowest-lying excited state is of ³LC nature and based on the EP moiety. However, it does not act as an “energy reservoir” for the higher-lying ³MLCT

[a] Laboratoire de Chimie Moléculaire, École de Chimie, Polymères, Matériaux (ECPM), Université Louis Pasteur (ULP), 25 rue Becquerel, 67087 Strasbourg Cedex 02, France
E-mail: ziessel@chimie.u-strasbg.fr

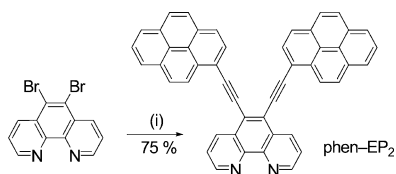
[b] Istituto per la Sintesi Organica e la Fotoreattività, Consiglio Nazionale delle Ricerche (ISOF-CNR), Via P. Gobetti 101, 40129 Bologna, Italy
E-mail: franz@isof.cnr.it

level(s); instead, the weak $^3\text{MLCT}$ emission that can be detected, both at room temperature ($f_{\text{em}} \approx 10^{-3}$) and at 77 K, is likely due to excitation trapping effects at the $\text{Ru}(\text{dpp})$ -based moiety of $[\text{Ru}(\text{dpp})_2(\text{phen-EP}_2)]^{2+}$ complex **1**.

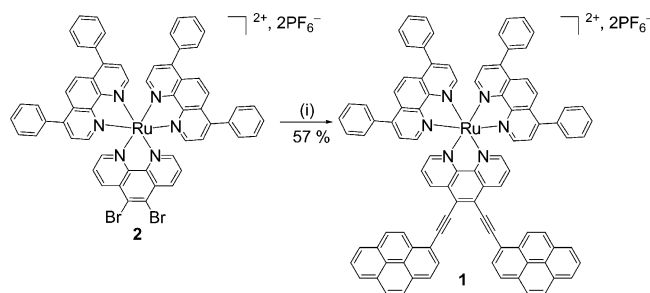
Results and Discussion

Synthesis

The phen-EP₂ ligand was conveniently prepared as sketched in Scheme 1 by using a palladium cross-coupling reaction between 1-ethynylpyrene and 5,6-dibromo-1,10-phenanthroline. Unfortunately, we were unable to prepare the ruthenium(II) complex of this ligand by a classical procedure, because phen-EP₂ proved to be poorly soluble in the required solvent. The problem was circumvented by the synthesis of pivotal starting complex **2**, which bears a disubstituted dibromophenanthroline framework (Scheme 2). This compound was obtained by coordination of 5,6-dibromo-1,10-phenanthroline to $[\text{Ru}(\text{dpp})_2\text{Cl}_2]$. This complex could then react smoothly in the employed solvent by using low-valent palladium(0) and 1-ethynylpyrene (2 equiv.) to provide desired pyrene substituted complex **1** in 57% yield.



Scheme 1. Reagents and conditions: (i) 1-ethynylpyrene, $\text{C}_6\text{H}_6/i\text{Pr}_2\text{NH}$, $\text{Pd}(\text{PPh}_3)_4$ (6 mol-%), 60 °C.



Scheme 2. Reagents and conditions: (i) 1-ethynylpyrene, $\text{CH}_3\text{CN}/\text{C}_6\text{H}_6$ (1:1), $i\text{Pr}_2\text{NH}$, $\text{Pd}(\text{PPh}_3)_4$ (6 mol-%), 60 °C.

The two complexes were unambiguously characterised by NMR, FAB^+ and FTIR spectroscopy and elemental analysis (see Experimental Section), and all data were consistent with the proposed structures. In particular, a weak band attributed to the $\text{C}\equiv\text{C}$ stretching vibration is observed at 2181cm^{-1} for the phen-EP₂ ligand and at 2180cm^{-1} for complex **1** in the FTIR spectra.

Electrochemistry

Electrochemical data are gathered in Table 1. The single-oxidation potential in complex **2** occurs at $E_{1/2} = +1.26\text{ V}$

vs. SCE and is attributed to $\text{Ru}^{\text{II}} \rightarrow \text{Ru}^{\text{III}}$ oxidation. This process is facilitated by 140 mV relative to that of $[\text{Ru}(\text{phen})_3]^{2+}$, which results from a balance of effects from the dibromophenanthroline and diphenylphenanthroline ligands; similar effects were previously observed in tetrasubstituted Ru^{II} -phenanthroline complexes.^[12,13] For pyrene-grafted complex **1**, this process is irreversible on the electrochemical timescale ($E_{1/2} = +1.35\text{ V}$ vs. SCE), presumably because of some overlap between the Ru- and pyrene-based oxidation steps given that oxidation of 1-ethynylpyrene is usually irreversible and occurs around +1.45 V vs. SCE.^[14] For both complexes, the subsequent reduction waves are ligand-based, as usually found for octahedral ruthenium(II) complexes.^[10] Comparison with the case of $[\text{Ru}(\text{phen})_3]$ ($E_{1/2} = -1.41\text{ V}$ vs. SCE; Table 1) suggests that the first reduction potential in complexes **1** and **2** ($E_{1/2} = -1.11$ and -1.23 V vs. SCE, respectively) can be attributed to the reduction of the 4,7-disubstituted-1,10-phenanthroline ligand. The 180 and 300 mV positive shift is likely due to the σ -electron-withdrawing effect of the bromo and ethynylpyrene substituents, respectively. For complex **1**, the higher degree of conjugation in the phenanthroline-ethynylpyrene ligand is also likely to favour a more-pronounced positive shift. Consistent with this, the fact that the first reduction in **1** takes place at a potential that is more positive than that of **2** might be taken as an indication that the LUMO of **1** is localised on the ethynyl-containing ligand.

Table 1. Electrochemical data for the Ru complexes.^[a]

	E_{ap} or $E_{1/2}$, V (ΔE , mV)	
2	+1.26 (70)	-1.23 (70), -1.40 (70) -1.57 (70)
1	+1.35 (irr) ^[b]	-1.11 (60), -1.39 (60), -1.60 (70), -1.75 (80) ^[c]
$\text{Ru}(\text{phen})_3^{2+}$ ^[d]	+1.40 (60)	-1.41 (60), -1.54 (60), -1.84 (70)

[a] Potentials determined by cyclic voltammetry at room temperature in 0.1 M TBAPF₆/CH₃CN solution, complex concentration ca. $3 \times 10^{-3}\text{ M}$. All potentials ($\pm 15\text{ mV}$) are reported in volts vs. SCE as reference electrode with the use of Fc^+/Fc (+0.38 V, $\Delta E = 60\text{ mV}$) as internal standard. Scan rate 200 mV s^{-1} . [b] E_{ap} (anodic peak potential) corresponds to an irreversible electrode process. [c] Double current intensity due to the reduction of the two ethynylpyrene appendages. [d] Ref.^[11]

The second reduction potential in both complexes **1** and **2** is very close to the first reduction potential of the $[\text{Ru}(\text{phen})_3]^{2+}$ complex,^[11] whereas the third reduction potential is close to the second reduction wave of $[\text{Ru}(\text{phen})_3]^{2+}$ (Table 1). For complex **1**, the additional cathodic potential ($E_{1/2} = -1.75\text{ V}$ vs. SCE) is assigned to the quasireversible reduction of both ethynylpyrene subunits. This last reduction step occurs with a twofold increase in the current intensity relative to that of the lowest cathodic reduction step due to close reduction of both pyrene residues. Such behaviour has also been observed for related complexes.^[14]

Optical Spectroscopy

The ground-state absorption spectra of **1**, the reference complex without the EP appendages [Ru(dpp)₂(phen-Br₂)²⁺ (**2**)] and of the phen-EP₂ ligand are displayed in Figure 1; spectroscopic data are collected in Table 2. In the region 270–280 nm, complex **1** shows ligand-based absorption features^[10] similar to those of **2**, apart from a slight redshift of the peak. This is an expected result^[12,13] given that the first coordination sphere of the two complexes is composed of the same number of (derivatised) phen chromophores, and the redshift of the absorption peak observed for **1** is ascribable to electronic delocalisation effects by the EP appendages. In the region 300–400 nm, **1** shows absorption characteristics not exhibited by **2**. As suggested by comparison with the absorption profile of phen-EP₂ (Figure 1, inset), the absorption peak for **1** with $\lambda_{\text{max}} = 364$ nm and $\epsilon = 49200 \text{ M}^{-1} \text{ cm}^{-1}$ is ascribable to ligand-localised transitions at the EP moiety. With regard to the range 400–550 nm, where ¹MLCT bands typically dominate in the absorption spectra of Ru^{II}-polypyridine complexes,^[10] the intensity of the band is found rather high for **1** ($\epsilon_{457} = 53700 \text{ M}^{-1} \text{ cm}^{-1}$) relative to those of **2** and [Ru(phen)₃]²⁺^[15] ($\epsilon_{443} = 27800 \text{ M}^{-1} \text{ cm}^{-1}$ and $\epsilon_{447} = 18400 \text{ M}^{-1} \text{ cm}^{-1}$, respectively). This could be due to known effects related to a large charge displacement, because the Ru→LCT event is likely to somehow involve the distant EP fragments.^[16] In ad-

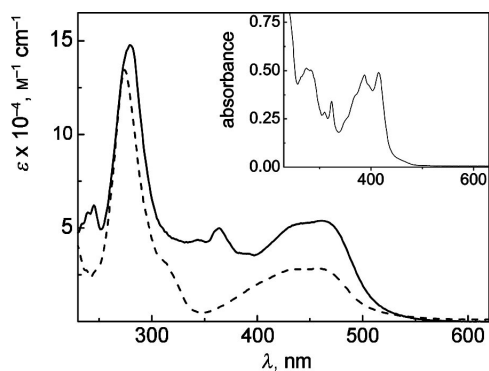


Figure 1. Ground-state absorption spectra in CH₃CN solutions of complexes **1** (full line) and **2** (dashed line). The inset shows the absorbance profile of the phen-EP₂ ligand in CH₂Cl₂.

Table 2. Absorption and luminescence properties.^[a]

	Absorption ^[b]	Emission ^[c] at 295 K				Emission ^[c] at 77 K	
	λ_{max} , nm (ϵ , M ⁻¹ cm ⁻¹)	λ_{em} , nm	f_{em}	τ_{em} , μs	k_{r} ^[d] , s ⁻¹	λ_{em} , nm	τ_{em} , μs
1	457 (53700)	607 (-) ^[f]	9×10^{-4} (-) ^[f]	4.5 ^[e] (-) ^[f]	200	590	7.9
2	443 (27800)	620	6.1×10^{-2} (1.2×10^{-2})	0.9 (0.18)	6.8×10^4	610	5.6
phen-EP ₂ ^[g]	415 ^[h]	480	6.5×10^{-2}	1.2×10^{-3} ^[i]	5.4×10^7	486	3.8×10^{-3}

[a] CH₃CN and CH₂Cl₂ solvent for the complexes and the free ligand, respectively. [b] Lowest-energy band. [c] Degassed samples, within brackets results for air-equilibrated cases; for the luminescence spectra, $\lambda_{\text{exc}} = 462$ and 415 nm for the complexes and the free ligand, respectively; for the luminescence lifetimes, $\lambda_{\text{exc}} = 465$ and 373 nm, respectively. [d] From $k_{\text{r}} = f_{\text{em}}/\tau_{\text{em}}$; for **1**, given the weak luminescence intensity the drawn k_{r} value may be subject to a large uncertainty. [e] From TA experiments $\tau_{\text{TA}} = 57 \mu\text{s}$; $\lambda_{\text{exc}} = 355$ nm, see text. [f] Not detected. [g] Luminescence properties are due to fluorescence unless otherwise stated. [h] Not determined due to low solubility. [i] From TA experiments, the ³LC level exhibits $\tau_{\text{TA}} = 28 \mu\text{s}$; $\lambda_{\text{exc}} = 355$ nm, see text.

dition, as suggested by the absorption tail of the phen-EP₂ ligand (Figure 1, inset), ¹LC transitions localised at the ethynylpyrene fragments or intraligand ethynylpyrene→phen CT (¹ILCT) transitions could be present in this range.^[17]

A summary of the luminescence properties for complexes **1** and **2** and the phen-EP₂ ligand is given in Table 2; λ_{exc} was 462 nm for the complexes and 415 nm for phen-EP₂. Figures 2 and 3 show the room temperature and 77 K luminescence spectra, respectively. For complex **2** at room temperature, the emission properties are typical of ³RuLCT emitters: $\lambda_{\text{em}} = 620$ nm, $f_{\text{em}} = 6.1 \times 10^{-2}$, $\tau_{\text{em}} = 0.9 \mu\text{s}$ and radiative rate constant, $k_{\text{r}} = 6.8 \times 10^4 \text{ s}^{-1}$, with $k_{\text{r}} = f_{\text{em}}/\tau_{\text{em}}$.^[10,12,13] In contrast, at room temperature, complex **1** is only weakly luminescent in O₂-free solvent with $\lambda_{\text{em}} = 607$ nm, $f_{\text{em}} = 9.0 \times 10^{-4}$, $\tau_{\text{em}} = 4.5 \mu\text{s}$ and $k_{\text{r}} = 200 \text{ s}^{-1}$. The k_{r} value for **2** is typical of ³MLCT emitters, whereas for **1** it is rather indicative of a ³LC emission.^[18] It is notable that in air-equilibrated solvent, **1** is not luminescent within the limits of detection (Table 2).

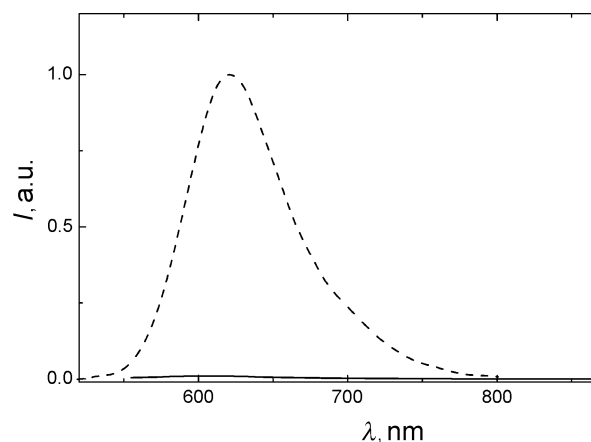


Figure 2. Luminescence spectra at room temperature of complexes **1** (full line) and **2** (dashed line) for isoabsorbing and degassed CH₃CN solutions; $\lambda_{\text{exc}} = 462$ nm.

Upon excitation at 355 nm, the room-temperature difference transient absorption (TA) spectra (Figure 4) for timescales up to 100 μs are observed for **1** and phen-EP₂. The TA spectrum of the ligand (Figure 4, top) is to be attributed to the lowest-energy ³LC (³ $\pi\pi$) level. After a 0.7 μs delay, it

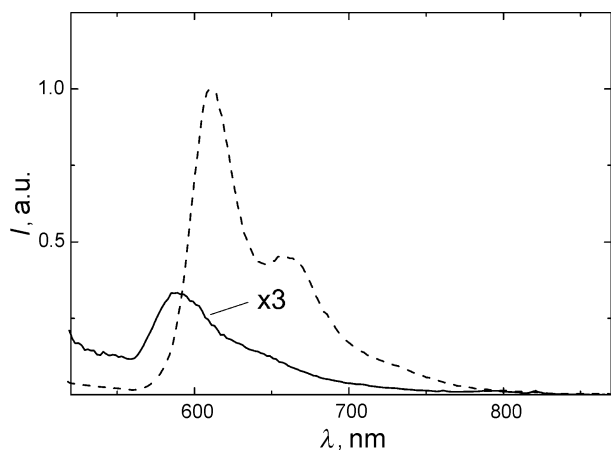


Figure 3. Luminescence spectra at 77 K of complexes **1** (full line) and **2** (dashed line) for roughly isoabsorbing and degassed CH_3CN solutions; $\lambda_{\text{exc}} = 462$ nm.

exhibits ground-state bleaching, which peaks at 380 nm, and therefore the spectrum matches the absorption profile appearing in the inset of Figure 1. Strong absorption features are registered for $\lambda > 450$ nm, and positive peaks are observed at 500 and 610 nm. The TA profile of phen-EP₂ differs somehow from that of neat pyrene, which shows positive peaks at 415 and 515 nm.^[19] This suggests that for phen-EP₂, the involved excited state is not fully localised at the pyrene unit, but rather it is spread to include the ethynyl

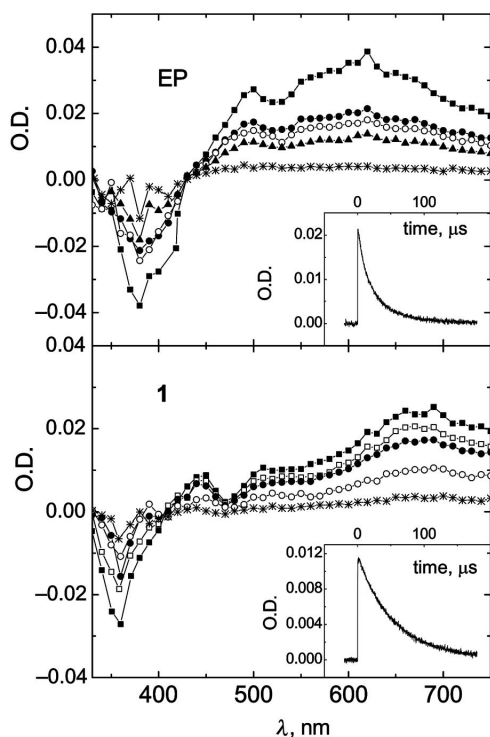


Figure 4. TA spectra at room temperature of the phen-EP₂ ligand (top: degassed CH_2Cl_2 solvent; delays: 0.7, 11, 14, 20, 57 μs) and complex **1** (bottom: degassed CH_3CN solvent; delays: 1, 12, 20, 45, 100 μs); $\lambda_{\text{exc}} = 355$ nm. The insets show the temporal decay of the band at 500 nm.

and/or phen fragments. The spectrum of phen-EP₂ decayed with $\tau = 28$ μs , as observed at 500 nm, whereas for the ³LC level of neat pyrene $\tau = 100$ μs ;^[18] for both cases the data was recorded in O₂-free CH_2Cl_2 .

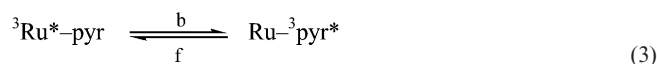
With regard to the TA spectrum of **1** (Figure 4, bottom; degassed AN solvent), after a 1 μs delay, the ground-state bleaching was found at 360 nm, which corresponds to the ground-state absorption peak of the EP component in this complex (Figure 1). In addition, broad absorption features were found at $\lambda > 450$ nm (peak at 690 nm), with a modest bump for some profiles at ca. 480 nm, which qualitatively matches previous observations for Ru^{II}-bpy systems containing pyrenylethylene subunits.^[20] The TA spectrum of **1** decayed with $\tau = 57$ μs as observed at 500 nm. All of this is consistent with a ³LC nature for the lowest-lying excited state of this complex.^[20] The presence of this level affects the luminescence behaviour of **1**, as described in the following.

For bichromophores based on $[\text{Ru}(\text{LL})_3]^{2+}$ and pyrene (pyr) moieties, $[\text{Ru}(\text{LL})_3]^{2+}$ -pyr_n (cases have been systematically explored with *n* in the range 1 to 6),^[21] the energy gap Δ_{TT} between ³Ru and lower-lying ³pyr levels was found to be a few hundred wavenumbers.^[5,6,19,22,23] As a consequence, at room temperature (295 K), thermal equilibration between these levels can be established according to Equation (1)

$$\frac{N_{\text{Ru}}}{N_{\text{pyr}}} = \exp\left(-\frac{\Delta_{\text{TT}}}{k_{\text{B}}T}\right) \quad (1)$$

where $N_{\text{Ru}}/N_{\text{pyr}}$ denotes the population ratio of the ³RuLCT and ³pyr states and Δ_{TT} is the energy gap between them; $k_{\text{B}}T = 205.9$ cm^{-1} (295 K). On this basis, the luminescence properties of such bichromophores can be understood with the help of Equations (2) and (3).^[21]

$$\phi_{\text{em}} = (1 - \alpha)\phi_{\text{Ru}} + \alpha\phi_{\text{pyr}} \quad (2)$$



According to the above Equations, the overall luminescence output f_{em} is regarded to originate from the balance of two localised contributions, $(1 - \alpha)$ and α , for the excited ³Ru* and ³pyr* states, respectively. The forward (f) and backward (b) energy-transfer steps are defined with reference to the employed excitation wavelength, $\lambda_{\text{exc}} = 355$ nm, so that predominant excitation of the pyr-containing EP unit takes place. Nevertheless, it should be noted that from the initially populated ¹pyr* level, both the ³pyr* and ³Ru* levels are independently accessed.^[6] Thermal equilibration is affected by the temperature, and below we discuss separately (i) room temperature and (ii) 77 K luminescence results, while having in mind that ethynylpyrene (EP) is an electronically more extended system than pyr.

At room temperature, a ³pyr-like level is typically non-emitting. This is due to its low radiative rate constant ($k_r < 10^3 \text{ s}^{-1}$).^[18] For bichromophores of the type [Ru(LL)₃]²⁺–pyr_n, a common observation is that only a ³MLCT Ru-based emission is present, and it typically exhibits $k_r \approx 10^5 \text{ s}^{-1}$.^[10] For such bichromophores, the ³pyr level only plays the role of “energy-reservoir”, provided its energy position is very close but slightly lower than that of the Ru-based emitter.^[5,6,19,22,23] In this case, upon effective thermal equilibration between the ³MLCT and ³pyr levels, the ³Ru-based luminescence is found to feature (a) the same intensity of the component complex alone and (b) a longer lifetime depending on α [Equation (2)].^[21] For the present bichromophore **1**, constituted by a [Ru(dpp)₃]²⁺ core and EP units (more electronically delocalised than pyr), the ³Ru-based luminescence intensity registered at room temperature in O₂-free solvent, is weaker by two orders of magnitude than that for complex **2** ($f_{\text{em}} = 9 \times 10^{-4}$ and 6.1×10^{-2} , respectively). This finding suggests that in **1**, thermal redistribution between the ³Ru* and ³EP* excited levels [Equations (1–3)], is not effective (it is largely displaced in favour of ³EP*), which might be a consequence of an energy gap that is too large between these levels ($\Delta_{TT} \gg k_B T$). Consistent with this, for air-equilibrated solvent, no luminescence is detected for **1** (Table 2), which indicates that deactivation of the long-lived lowest-lying ³LC level (57 μs , see above) by O₂ diffusional quenching successfully competes against the forward transfer [Equation (3)].

On passing from room temperature to 77 K, a blueshift of the emission peak is registered for **2** and λ_{em} moves from 620 to 610 nm. This is an expected behaviour for CT emitters upon going from fluid to frozen polar solvents.^[10] At 77 K, **1** is also luminescent, with $\lambda_{\text{max}} = 590 \text{ nm}$ and a detected luminescence intensity that is ca. 0.1 times that of **2** (Figure 3). On the basis of the emission profiles (Figure 3) and lifetimes ($\tau = 7.9$ and 5.6 μs for **1** and **2**, respectively; Table 1), the 77 K results indicate a ³MLCT nature for the emission in both cases. At low temperatures, the $N_{\text{Ru}}/N_{\text{pyr}}$ ratio is expected to be much smaller than that at room temperature, and the observed ³MLCT nature for the 77 K emission of **1** cannot be explained in terms of thermal equilibration [Equations (1–3)], which is already not effective at room temperature.

An explanation for the low temperature observations might rely on the heteroleptic nature of complex **1** as opposed to the homoleptic cases. Actually, for the equivalent ligands of a homoleptic system and according to an interligand hopping model for the ligand-localised description of the ³M←L CT event,^[10] the observed emission properties are obviously independent of the individual ligand bearing the ³MLCT excitation (i.e., the excess electron).^[10,24] This is also the case at 77 K, where interligand hopping of the excess electron of the luminescent ³MLCT state is severely limited (a hopping barrier of the order of 700–900 cm^{-1} may be evaluated),^[25] but the emission is in any circumstance centred on one of the equivalent ligands. In contrast, for a heteroleptic system of the type [Ru(LL_a)₂(LL_b)]²⁺, ¹MLCT states involving the individual LL_a or LL_b ligands

are populated upon light absorption. Under these circumstances, low-temperature single-ligand electron trapping may result in different emission properties, depending on which ligand, LL_a or LL_b, is bearing the excess electron. In particular, whereas ³M←L CT states localised at the phen–EP₂ ligand could undergo deactivation by low-lying practically nonluminescent ³pyr-like levels localised on the EP moieties, the weak ³MLCT luminescence observed at 77 K for **1** ($\lambda_{\text{em}} = 590 \text{ nm}$, $\tau_{\text{em}} = 7.9 \mu\text{s}$) might be ascribable to ³M←L CT states localised (entrapped) on one of the dpp ligands.

Experimental Section

General Methods: The ¹H and ¹³C NMR spectra were recorded at room temperature with a Bruker AC 200 MHz, a Bruker Avance 400 MHz or a Bruker Avance 300 MHz spectrometer with the use of perdeuterated solvents as internal standard: δ_{H} in ppm relative to residual proton in the solvents (not 100% deuteriated); δ_{C} in ppm relative to the solvent. FTIR spectra were recorded as KBr pellets. Absorption spectra were recorded in CH₂Cl₂ or CH₃CN with a UVIKON 933 absorption spectrometer. Fast atom bombardment (FAB, positive mode) mass spectra were recorded with a ZAB-HF-VB-analytical apparatus with *m*-nitrobenzyl alcohol (*m*-NBA) as matrix. Electrospray (ES) mass spectra were recorded with a 1100 MSD Hewlett Packard spectrometer. Electrochemical studies employed cyclic voltammetry with a conventional three-electrode system by using a BAS CV-50W voltammetric analyser equipped with a Pt disk (2 mm²) working electrode and a silver wire counter-electrode. Ferrocene was used as an internal standard and was calibrated against a saturated calomel reference electrode (SCE) separated from the electrolysis cell by a glass frit presoaked with electrolyte solution. Solutions contained the electroactive substrate in deoxygenated and anhydrous dichloromethane or acetonitrile containing doubly recrystallised tetra-*n*-butylammonium hexafluorophosphate (0.1 M) as supporting electrolyte. The quoted half-wave potentials were reproducible within $\approx 15 \text{ mV}$.

Materials: 1-Ethynylpyrene,^[14] *cis*-[Ru(4,7-diphenyl-1,10-phenanthroline)₂Cl₂],^[26] [Pd(PPh₃)₄]^[27] and 5,6-dibromo-1,10-phenanthroline^[28] were prepared and purified according to literature procedures. Diisopropylamine and acetonitrile were dried with suitable reagents and distilled under an atmosphere of argon immediately prior to use. CH₂Cl₂ and *i*Pr₂NH were distilled from P₂O₅ and KOH, respectively.

5,6-Bis(1-ethynylpyrene)-1,10-phenanthroline (phen–EP₂): A Schlenk flask equipped with a septum, a Teflon-coated magnetic stirring-bar and an argon inlet was charged with 5,6-dibromo-1,10-phenanthroline (100 mg, 0.30 mmol) and 1-ethynylpyrene (81 mg, 0.36 mmol) in argon-degassed benzene/*i*Pr₂NH (20:2 mL), and finally Pd(PPh₃)₄ (21 mg, 6% mol) was added as a solid. The solution was heated at 60 °C, until complete consumption of the starting material was determined by TLC. After cooling, the precipitate was filtered and washed with water (2 × 20 mL) and diethyl ether (2 × 10 mL). The analytically pure compound was recovered without any additional treatment (141 mg, 75%). Because of its insolubility, NMR spectra were not obtained. IR (KBr): $\tilde{\nu} = 2912 \text{ (m)}$, 2850 (m), 2181 (m), 1619 (s), 1595 (s), 1432 (s), 1261 (m), 1096 (m), 876 (m), 844 (m), 716 (m) cm^{-1} . MS (ESI, CH₂Cl₂): $m/z = 629.2$ [M + H]⁺. C₄₈H₂₄N₂ (628.73): calcd. C 91.70, H 3.85, N 4.46; found C 91.51, H 3.57, N 4.82.

[Ruthenium(II)(4,7-diphenyl-1,10-phenanthroline)₂(5,6-dibromo-1,10-phenanthroline)](PF₆)₂ (2): In a Schlenk flask containing a stirred ethanol/water (10:1 mL) solution of *cis*-[Ru(4,7-diphenylphenanthroline)₂]Cl₂ (0.1 g, 0.13 mmol) was added the 5,6-dibromophenanthroline ligand (0.05 g, 0.15 mmol). The mixture was heated for 16 h at 80 °C until complete consumption of the starting material was observed. After cooling, the solution was filtered, potassium hexafluorophosphate in water was added, and the solution was evaporated. The crude precipitate was washed with water (2×) and diethyl ether (1×), and it was then chromatographed on a column packed with alumina (MeOH/CH₂Cl₂, gradient 0:100 to 2:98). The fractions containing the pure complex were evaporated to dryness and recrystallised by slow evaporation of CH₂Cl₂ from a mixture of CH₂Cl₂/hexanes (approximately 80:20). Recrystallisation gave 120 mg (66%) of analytically pure product. ¹H NMR (300 MHz, [D₆]acetone, 20 °C): δ = 9.02 (dd, ³J = 8.7 Hz, ⁴J = 1.1 Hz, 2 H), 8.65 (dd, ³J = 5.3 Hz, ⁴J = 1.0 Hz, 2 H), 8.61 (d, ³J = 5.5 Hz, 2 H), 8.57 (d, ³J = 5.5 Hz, 2 H), 8.33 (s, 4 H), 7.98 (dd, ³J = 8.7 Hz, ³J = 5.3 Hz, 2 H), 7.79 (d, ³J = 5.6 Hz, 2 H), 7.75 (d, ³J = 5.6 Hz, 2 H), 7.65–7.63 (m, 20 H) ppm. ¹³C{¹H} NMR (75 MHz, [D₆]acetone, 20 °C): δ = 154.9, 153.9, 153.7, 150.2, 150.1, 149.65, 149.60, 149.1, 138.4, 136.65, 136.63, 132.0, 130.8, 130.7, 130.6, 130.04, 129.93, 129.87, 128.6, 127.3, 127.2, 127.1 ppm. FTIR (KBr): ν̄ = 3437 (m), 3058 (m), 2919 (m), 1622 (m), 1594 (m), 1444 (m), 1417 (s), 1116 (m), 1096 (m), 836 (s), 765 (m), 702 (m) cm⁻¹. UV/Vis (CH₃CN): λ (ε, M⁻¹cm⁻¹) = 443 (27800), 273 (142300) nm. MS: (ESI, CH₃CN): *m/z* = 1249.2 [M - PF₆]⁺. C₆₀H₃₈Br₂F₁₂N₆P₂Ru (1393.80): calcd. C 51.70, H 2.75, N 6.03; found C 51.45, H 2.39, N 5.71.

[Ruthenium(II)(4,7-diphenyl-1,10-phenanthroline)₂(5,6-{1-ethynylpyrene}-1,10-phenanthroline)](PF₆)₂ (1): In a Schlenk flask containing a stirred degassed acetonitrile/benzene solution (1.5:1.5 mL) of [ruthenium(II)(4,7-diphenyl-1,10-phenanthroline)₂(5,6-dibromo-1,10-phenanthroline)](PF₆)₂ (30 mg, 0.021 mmol) was sequentially added [Pd(PPh₃)₄] (2 mg, 6 mol-%), diisopropylamine (0.5 mL) and 1-ethynylpyrene (12 mg, 0.054 mmol). The mixture was heated under an atmosphere of argon for 16 h until the complete consumption of the starting material was observed. The solution was cooled to room temperature and potassium hexafluorophosphate in water was added, and the solvent was evaporated. The crude precipitate was washed with water (2×) and diethyl ether (1×), and it was chromatographed on a column packed with silica gel (acetonitrile/water/aqueous saturated KNO₃, 85:15:0 to 85:15:0.2). After anionic exchange, the analytically pure compound was obtained after recrystallisation from dichloromethane/hexane (20 mg, 57%). ¹H NMR (300 MHz, [D₆]acetone, 20 °C): δ = 8.84 (d, ³J = 9.0 Hz, 2 H), 8.76 (d, ³J = 5.5 Hz, 2 H), 8.72–8.69 (m, 4 H), 8.61 (d, ³J = 8.1 Hz, 2 H), 8.40 (d, ³J = 8.1 Hz, 2 H), 8.38 (s, 4 H), 8.34–8.24 (m, 8 H), 8.08 (dd, ³J = 8.5 Hz, ⁴J = 5.2 Hz, 2 H), 8.03–7.91 (m, 4 H), 7.87 (d, ³J = 5.6 Hz, 2 H), 7.84 (d, ³J = 5.5 Hz, 2 H), 7.70–7.73 (m, 20 H), 7.60 (d, ³J = 9.2 Hz, 2 H) ppm. ¹³C{¹H} NMR (75 MHz, [D₆]acetone, 20 °C): δ = 152.8, 149.3, 148.8, 148.1, 135.7, 131.2, 130.70, 130.66, 129.89, 129.85, 129.7, 129.34, 129.26, 129.17, 129.0, 127.2, 126.7, 126.4, 126.2, 126.1, 124.9, 115.7, 90.2 (C_{ethynyl}) ppm. FTIR (KBr): ν̄ = 3436 (m), 3143 (m), 2922 (m), 2853 (m), 2513 (m), 2180 (m), 1620 (s), 1595 (s), 1428 (s), 1186 (m), 1120 (m), 837 (s), 703 (m) cm⁻¹. UV/Vis (CH₃CN): λ (ε, M⁻¹cm⁻¹) = 457 (53700), 435 (52000), 361 (50000), 277 (155300), 232 (122900) nm. MS: (ESI, CH₃CN): *m/z* = 1539.2 [M - PF₆]⁺. C₉₆H₅₆F₁₂N₆P₂Ru (1684.53): calcd. C 68.45, H 3.35, N 4.99; found C 68.22, H 3.09, N 4.75.

Optical Spectroscopy: UV/Vis absorption spectra of the ligand and of the complexes in CH₂Cl₂ and CH₃CN, respectively, were ob-

tained with Uvikon 933 or Perkin–Elmer Lambda 45 spectrometers; the ligand was poorly soluble and only its absorbance profile was obtained. The luminescence spectra of O₂-free or air-equilibrated solutions at room temperature (absorbance < 0.15 at the excitation wavelength) and at 77 K were measured with a Spex Fluorolog II spectrofluorometer with an excitation wavelength of 415 and 462 nm for the ligand and the complexes, respectively. Degassing of the samples was accomplished by argon bubbling or freeze–pump cycling in a vacuum line. Corrected luminescence spectra were obtained by using a correction curve for the phototube response provided by the manufacturer. Luminescence quantum efficiencies (*f_{em}*) were evaluated by comparing wavelength-integrated intensities (*I*) with reference to [Ru(bpy)₃]Cl₂ (*f_r* = 0.028, air-equilibrated water)^[29] and by using Equation (4):^[30]

$$\phi_{em} = \frac{A_r \eta^2 I}{\eta_r^2 I_r A} \phi_r \quad (4)$$

where *A* and *η* are the absorbance value (<0.15) at the employed excitation wavelength and the refractive index of the solvent, respectively. Band maxima and relative luminescence intensities are obtained with uncertainty of 2 nm and 20%, respectively. The luminescence lifetimes of the complexes were obtained with an IBH 5000F single-photon equipment by using nanoled excitation sources at 373 and 465 nm, for the ligand and complexes, respectively. Analysis of the luminescence decay profiles against time was accomplished by using software provided by the manufacturers. Estimated errors are 10% on lifetimes, and the working temperature was either 295 ± 2 K (1-cm square optical cells employed) or 77 K (with samples contained in capillary tubes immersed in liquid nitrogen). Transient absorption (TA) spectra for degassed solutions were observed in the microsecond time domain by using a Proteus nanosecond flash photolysis apparatus by Ultrafast Systems LLC.^[31] The excitation from a Continuum Surelite II Nd:YAG laser was at 355 nm (5-ns pulse duration, 5 mJ per pulse). The probe light source was a Spectra Physics 69907 150-W continuous wave Xe arc lamp. Light signals were passed through a Chromex/Bruker 250IS monochromator and collected with a high-speed Silicon DET210 Thorlabs detector. After signal amplification by a Femto DHPVA-200 variable-gain wideband voltage amplifier and registration at a Tektronix TDS 3032 B digital oscilloscope, treatment of the signals was performed with the help of acquisition software by Proteus; to extract lifetimes, the temporal decay of the TA band at 500 nm was monitored.

Acknowledgments

The authors thank CNRS and IST/ILO (Contract 2001-33057) for funding and acknowledge support from Consiglio Nazionale delle Ricerche, Italy (Project MACOL PM.P04.010). Professor F. N. Castellano from the University of Bowling Green State University in the USA is also acknowledged for providing us with a sample of 5,6-dibromo-1,10-phenanthroline.

- [1] J. H. Alstrum-Acevedo, M. K. Brennaman, T. J. Meyer, *Inorg. Chem.* **2005**, *44*, 6802–6827.
- [2] V. Balzani, A. Juris, M. Venturi, S. Campagna, S. Serroni, *Chem. Rev.* **1996**, *96*, 759.
- [3] A. Harriman, R. Ziessel, *Chem. Commun.* **1996**, 1707–1716.
- [4] N. D. McClenaghan, Y. Leydet, B. Maubert, M. T. Indelli, S. Campagna, *Coord. Chem. Rev.* **2005**, *249*, 1336–1350.

- [5] D. S. Tyson, K. B. Henbest, J. Bialecki, F. N. Castellano, *J. Phys. Chem. A* **2001**, *105*, 8154–8161.
- [6] A. F. Morales, G. Accorsi, N. Armaroli, F. Barigelletti, S. J. A. Pope, M. D. Ward, *Inorg. Chem.* **2002**, *41*, 6711–6719.
- [7] P. C. Alford, M. J. Cook, A. P. Lewis, G. S. G. McAuliffe, V. Skarda, A. J. Thomson, J. L. Glasper, D. J. Robbins, *J. Chem. Soc. Perkin Trans. 2* **1985**, 705–709.
- [8] M. J. Cook, A. J. Thomson, *Chem. Br.* **1984**, *20*, 914–917.
- [9] V. Skarda, M. J. Cook, A. P. Lewis, G. S. G. McAuliffe, A. J. Thomson, D. J. Robbins, *J. Chem. Soc. Perkin Trans. 2* **1984**, 1309–1311.
- [10] A. Juris, V. Balzani, F. Barigelletti, S. Campagna, P. Belser, A. von Zelewsky, *Coord. Chem. Rev.* **1988**, *84*, 85–277.
- [11] A. Kirsch-De Mesmaeker, R. Nasielski-Hinkens, D. Maetens, D. Pauwels, J. Nasielski, *Inorg. Chem.* **1984**, *23*, 377–379.
- [12] S. Rau, R. Fischer, M. Jäger, B. Schäfer, S. Meyer, G. Kreisel, H. Gorls, M. Rudolf, W. Henry, J. G. Vos, *Eur. J. Inorg. Chem.* **2004**, 2001–2003.
- [13] B. Schäfer, H. Gorls, S. Meyer, W. Henry, J. G. Vos, S. Rau, *Eur. J. Inorg. Chem.* **2007**, 4056–4063.
- [14] M. Hissler, A. Harriman, A. Khatyr, R. Ziessel, *Chem. Eur. J.* **1999**, *5*, 3366–3381.
- [15] R. C. Young, T. J. Meyer, D. G. Whitten, *J. Am. Chem. Soc.* **1976**, *98*, 286–287.
- [16] C. C. Phifer, D. R. McMillin, *Inorg. Chem.* **1986**, *25*, 1329–1333.
- [17] C. Ringenbach, A. De Nicola, R. Ziessel, *J. Org. Chem.* **2003**, *68*, 4708–4719.
- [18] M. Montalti, A. Credi, L. Prodi, M. T. Gandolfi, *Handbook of Photochemistry*, 3rd ed., CRC Press, Taylor & Francis, Boca Raton, **2006**.
- [19] W. E. Ford, M. A. J. Rodgers, *J. Phys. Chem.* **1992**, *96*, 2917–2920.
- [20] D. V. Kozlov, D. S. Tyson, C. Goze, R. Ziessel, F. N. Castellano, *Inorg. Chem.* **2004**, *43*, 6083–6092.
- [21] N. D. McClenaghan, F. Barigelletti, B. Maubert, S. Campagna, *Chem. Commun.* **2002**, 602–603.
- [22] J. A. Simon, S. L. Curry, R. H. Schmehl, T. R. Schatz, P. Piotrowiak, X. Q. Jin, R. P. Thummel, *J. Am. Chem. Soc.* **1997**, *119*, 11012–11022.
- [23] G. J. Wilson, A. Launikonis, W. H. F. Sasse, A. W. H. Mau, *J. Phys. Chem. A* **1997**, *101*, 4860–4866.
- [24] N. H. Damrauer, T. R. Boussie, M. Devenney, J. K. McCusker, *J. Am. Chem. Soc.* **1997**, *119*, 8253–8268.
- [25] D. E. Morris, K. W. Hanck, M. K. Dearmond, *J. Am. Chem. Soc.* **1983**, *105*, 3032–3038.
- [26] G. Sprintschnik, H. W. Sprintschnik, P. P. Kirsch, D. G. Whitten, *J. Am. Chem. Soc.* **1977**, *99*, 4947–4954.
- [27] D. R. Coulson, *Inorg. Synth.* **1972**, *13*, 121.
- [28] M. Q. Feng, K. S. Chan, *Organometallics* **2002**, *21*, 2743–2750.
- [29] K. Nakamaru, *Bull. Chem. Soc. Jpn.* **1982**, *55*, 2967.
- [30] J. N. Demas, G. A. Crosby, *J. Phys. Chem.* **1971**, *75*, 991.
- [31] N. Armaroli, G. Accorsi, J. N. Clifford, J. F. Eckert, J. F. Nierengarten, *Chem. Asian J.* **2006**, *1*, 564–574.

Received: October 11, 2007

Published Online: January 15, 2008